Renewable Energy 69 (2014) 242–252

Contents lists available at ScienceDirect

Renewable Energy

journal homepage: www.elsevier.com/locate/renene

Electrodeposition and sol–gel derived nanocrystalline N–ZnO thin films for photoelectrochemical splitting of water: Exploring the role of microstructure

Nirupama Singh [b], Babita Kumari [b], Shailja Sharma [b], Surbhi Chaudhary [b], Sumant Upadhyay [b], Vibha R. Satsangi [a], Sahab Dass [b], Rohit Shrivastav [b,*]

[a] Department of Physics & Computer Science, Dayalbagh Educational Institute, Dayalbagh, Agra 282 110, India
[b] Department of Chemistry, Dayalbagh Educational Institute, Dayalbagh, Agra 282 110, India

ARTICLE INFO

Article history:
Received 28 June 2013
Accepted 24 March 2014
Available online

Keywords:
photoelectrochemical
nanomaterials
zinc oxide
nitrogen incorporation
water splitting
hydrogen

ABSTRACT

Nanocrystalline thin films of nitrogen (N)-incorporated ZnO, deposited on glass substrate by sol–gel (SG) and electrodeposition (ED) routes, have been investigated for their possible relevance to photoelectrochemical (PEC) splitting of water. XRD pattern established dominant evolution of hexagonal wurtzite ZnO. SEM analysis indicated continuous and homogenous growth of particles, while AFM analysis revealed favored growth of nanocrystallites along the *c*-axis. SG-derived films were denser with reduced film thickness. ED-derived samples were fluffy with relatively rougher top surface. All the samples exhibited broad absorption threshold at ~400 nm with only marginal dip to the band gap on N incorporation. By comparing the performance of SG- and ED-derived samples, results of the study highlight crucial role of semiconductor microstructure, viz. film thickness, density, particle size and distribution, and film surface characteristics on their PEC response.

1. Introduction

Zinc oxide (ZnO), a key technological material, has attracted many researchers in recent years for hydrogen generation via photoelectrochemical (PEC) splitting of water [1–5]. Despite its large band gap (~3.2 eV) restraining the absorption of dominantly present visible component of solar energy, the interest in ZnO mainly emanates from its high electron mobility, effectual charge separation, and well aligned band edges [6]. ZnO, like several other wide band gap semiconductors generate high photovoltage but low photocurrent. On the other hand, the smaller band gap semiconductors generate high photocurrent by utilizing larger fraction of the incident photons, but yield only insufficient voltage for photosplitting of water.

Impurity doping has been investigated vigorously in the past as a method to extend the absorption spectrum of ZnO to visible regions. However, compared to more extensively studied cation doping, doping by anion is still an intriguing phenomenon. Nitrogen, with its low ionization energy, comparable ionic radius (0.75 Å, compared to 0.72 Å for Zn and 0.73 Å for O), source abundance and ease of handling, is a promising anion dopant for producing shallow acceptor level in ZnO. Sudhakar et al. observed significant reduction in band gap of ZnO films prepared by RF sputtering on N doping [7]. Further, they found that as the RF power is increased from 100 to 300 W, both the magnitude of reduction in band gap and the crystallinity in samples increased. Reporting incident photon-to-current-efficiencies of PEC cell with ZnO:N nanowire arrays as photoanodes, Yang et al. also observed that N substitution at O sites in ZnO nanowires up to ~4% leads to significant increase in photoresponse in the visible region [8]. Qiu et al. investigated the effect of N doping on branched ZnO nanotetrapods for PEC splitting of water and recorded significant increase in photocurrent density on N doping, which they attributed primarily to band gap narrowing [9]. However, besides band gap reduction, other microstructural characteristics are also acquiescent to change on impurity incorporation. Doping-induced such alterations in microstructure, viz. particle size, density, porosity, electrical resistance, and film surface morphology and topography, and their effects on PEC behavior of nanostructured materials, is yet poorly understood. Past experience suggests that microstructural properties of semiconductor depend heavily on their preparation/synthesis protocol [10].

* Corresponding author.
E-mail address: rohitshrivastav_dei@yahoo.co.in (R. Shrivastav).

http://dx.doi.org/10.1016/j.renene.2014.03.042
0960-1481/

Table 1
Observed values of dislocation density (δ), microstrain (ε), root mean square (RMS) surface roughness and band gap energy (E_g).

	Nitrogen incorporation (% at.)	$(\delta) \times 10^{-14}$ (line^2/m^2)	$(\varepsilon)\ 10^{-3}$	RMS surface roughness (nm)	E_g (eV)
SG-derived	–	8.23	0.99	3	3.24
	0.5	8.36	1.02	5	3.24
	1.0	6.82	0.90	3	3.23
	2.0	6.76	0.90	4	3.23
	3.0	9.16	1.04	4	3.22
	5.0	11.49	1.17	3	3.22
	7.0	11.09	1.15	3	3.21
ED-derived	–	4.3	0.69	15	3.23
	0.5	4.7	0.75	20	3.22
	1.0	8.2	0.89	14	3.22
	2.0	5.6	0.82	13	3.21
	3.0	4.0	0.69	12	3.19
	5.0	4.7	0.75	12	3.16
	7.0	4.5	0.73	11	3.15

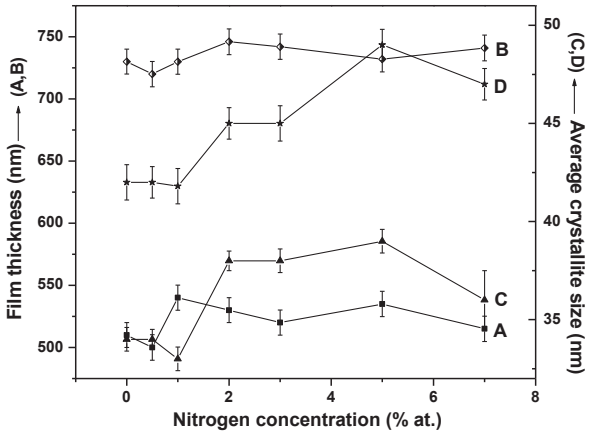

Fig. 2. Film thickness and average crystallite size (SG-derived: A and C; ED-derived: B and D).

In continuation to our previous works on doped/undoped ZnO films [1–4], the present study deals with the synthesis of nitrogen (N) incorporated thin films of nanocrystalline ZnO, grown over ITO plates, by two different techniques, sol–gel/spin-coating (SG) and electrodeposition (ED), for PEC splitting of water. Characterization of samples by XRD, SEM and AFM analysis suggests significant microstructural variations in the two sets of samples with impinging repercussions on their PEC performance. The study highlights that the reduction (or otherwise) in the band gap of wide band gap semiconductors on doping cannot be the sole criteria to evaluate their suitability for PEC splitting of water. Other associated microstructural changes are equally imperative and also need to be optimized for efficient PEC splitting of water.

2. Experimental

2.1. Thin film synthesis by sol–gel

To the solution of zinc acetate di-hydrate (prepared in di-methyl formamide, DMF) calculated quantity of urea was slowly added and the content was stirred for 3 h at 33 ± 2 °C. The resulting solution was spin coated (at 2500 rpm) on ITO sheets (1 cm × 1 cm) using a photoresist spinner. The ITO sheets were pre-washed by soaking for ~2 min in detergent solution followed by washing with double-distilled-deionized water. Subsequently, these were dripped for ~10 s in 0.1 M HCl, rinsed with water and acetone, and air-dried. The films were deposited layer-by-layer for five successive layers [2]. Each layer was dried in air at 50 °C for 10 min before the deposition of next layer over it. After the final deposition, the films were sintered in air at 250 °C for 30 min to remove organic contaminants. Afterwards, these were sintered in air at 600 °C for 60 min and cooled slowly for 24 h to complete the crystallization cycle. The films, thus obtained, were dip coated (for two successive layers at a rate of 10 s per dip) with a solution of zinc nitrate and hexamethylenetetramine (HMT) prepared in DMF. Coated films were dried at 50 °C on a hot plate and re-sintered in air at 600 °C for 60 min.

2.2. Thin film synthesis by electrodeposition

Pre-cleaned ITO sheets (1 cm × 1 cm) were used as working electrode, in conjunction with saturated calomel reference electrode and platinum auxiliary electrode. Aqueous solution of zinc nitrate mixed with potassium chloride (KCl) and ethylene-di-amine (EDA), calculated quantity of urea was added and used as electrolyte and kept under constant stirring. Electrochemical work station (ECDA-001, Conserv Enterprises) was employed to obtain films under CV mode (voltage range −1 to +1 V, temperature 80 °C) [11]. The deposited films were washed in a gentle flow of water and dried at 50 °C over hot plate and sintered at 250 °C for 30 min and at 600 °C for 1 h for proper crystallization. Sintering led to the

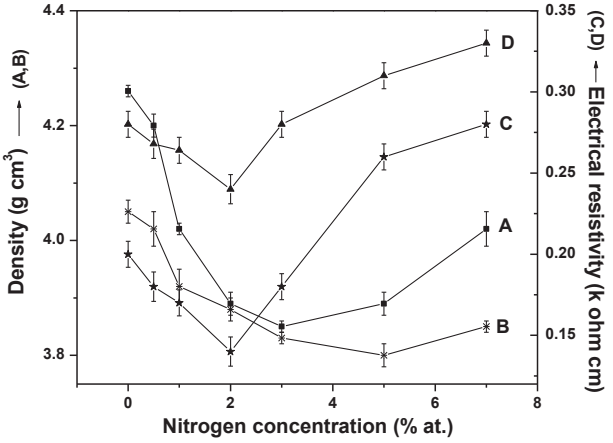

Fig. 1. Density and electrical resistivity of films (SG-derived: A and C; ED-derived: B and D).

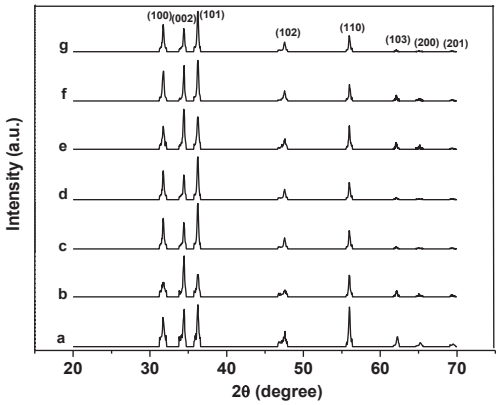

Fig. 3. XRD pattern of SG-derived films prepared with N concentration: nil (a), 0.5% at. (b), 1.0% at. (c), 2.0% at. (d), 3.0% at. (e), 5.0% at. (f) and 7.0% at. (g).